

Surface-based Manipulation Using Tunable Compliant Porous-Elastic Soft Sensing

Gayatri Indukumar^{1,2}, Muhammad Awais^{1,3}, Diana Cafiso¹, Matteo Lo Preti⁴, Lucia Beccai¹

Abstract—There is a growing need for soft robotic platforms that perform gentle, precise handling of a wide variety of objects. Existing surface-based manipulation systems, however, lack the compliance and tactile feedback needed for delicate handling. This work introduces the COmpliant Porous-Elastic Soft Sensing (COPESS) integrated with inductive sensors for adaptive object manipulation and localised sensing. The design features a tunable lattice layer that simultaneously modulates mechanical compliance and sensing performance. By adjusting lattice geometry, both stiffness and sensor response can be tailored to handle objects with varying mechanical properties. Experiments demonstrate that by easily adjusting one parameter, the lattice density, from 7% to 20%, it is possible to significantly alter the sensitivity and operational force range (about $-23\times$ and $9\times$ respectively). This approach establishes a blueprint for creating adaptive, sensorized surfaces where mechanical and sensory properties are co-optimized, enabling passive, yet programmable, delicate manipulation.

I. INTRODUCTION

Soft handling systems offer a promising tool for expanding the applications of soft robotics to various areas, such as the food and packaging industry, through their ability to transport and manipulate fragile and heterogeneous objects [1]. There are several examples of flexible surfaces, where the surface is deformed by actuation mechanisms. Different approaches are based on bellow-like modules, electrostatically driven actuators [2], bioinspired dynamic deformation [3], and pulley-and-belt-based linear actuators [4]. Despite advances in actuation and manipulation to move heterogeneous objects, these systems often lack adequate sensing. Among the few sensorized examples, ArrayBot [5] deploys commercial force resistive sensors, and [6] uses vision to track the geometric center position and orientation of objects. Nevertheless, opportunities remain to advance embedded sensorization in these systems. Tactile sensors present an excellent fit as they offer information regarding contact location, pressure distribution, object shape, and surface texture. Tactile sensors have seen a lot of advancements in recent years, exploiting various transduction approaches [7], [8]. In this work, inductive soft sensors are selected because

they balance sensitivity [9], spatial resolution, and cost-effectiveness [10], and are relatively insensitive to dust and moisture, making them well-suited for large-scale modular robotic systems in fields such as food manipulation and packaging [11].

Among soft inductive tactile sensors, a variety of modulating layers are used. The most common choice is to use an elastomer like Polydimethylsiloxane (PDMS) or EcoFlex [12], eventually combined with conductive fillers [13], [14]. Using a porous material represents another strategy to decrease the stiffness of the soft modulating layer. Porosity can be introduced via chemical routes [15], or by using commercial foams. In a previous work, we used a commercial polyurethane foam as the modulating layer [16]. Although commercial foams are readily available and well-suited for application-driven studies, their mechanical properties cannot be tuned on demand. A practical compromise between tunability and rapid iteration is offered by 3D-printed lattices, which support fast prototyping across multiple designs.

To address these challenges, we propose an approach that combines the environmental robustness of inductive sensing with the rapid design exploration offered by 3D-printed lattices. By integrating these two technologies, we create the COPESS, a robust tactile surface capable of handling a wide variety of delicate and deformable objects. Building the layer with a gradient stiffness provides a smooth surface that delicately embeds objects, enabling precise tuning of the force-detection range and the potential to optimize manipulation along defined patterns. The main contributions of this work are summarized as:

- The investigation of 3D-printed gyroid lattices as a tunable modulating element for inductive tactile sensors.
- A comprehensive characterization demonstrating the co-modulation of mechanical stiffness and sensing range.
- A proof-of-concept demonstration that our approach can be used, in the future, for passive object guidance using programmed stiffness gradients.

II. DESIGN

Figure 1 shows the proposed scheme and a breakdown of the COPESS. It consists of three layers:

- Copper and ferrite are used as target layers in the inductive sensor, with copper placed close to the coil to generate strong eddy currents and ferrite positioned behind it to guide the magnetic flux and reduce leakage [17]. This configuration enhances inductance variation, improves sensitivity, and minimizes external interference.

¹Gayatri Indukumar, Muhammad Awais, Diana Cafiso, and Lucia Beccai are with Soft BioRobotics Perception Group at Istituto Italiano di Tecnologia, 16163, Genova, Italy

²Gayatri Indukumar is also with the University of Genoa, 16126, Genova, Italy

³Muhammad Awais is also with the Biorobotics Institute, Scuola Superiore Sant'Anna, Pontedera, 56025, Italy

⁴Matteo Lo Preti is with the Soft Robotics Lab, National University of Singapore, 117575, Singapore

Corresponding Author: Lucia Beccai(email: Lucia.Beccai@iit.it)

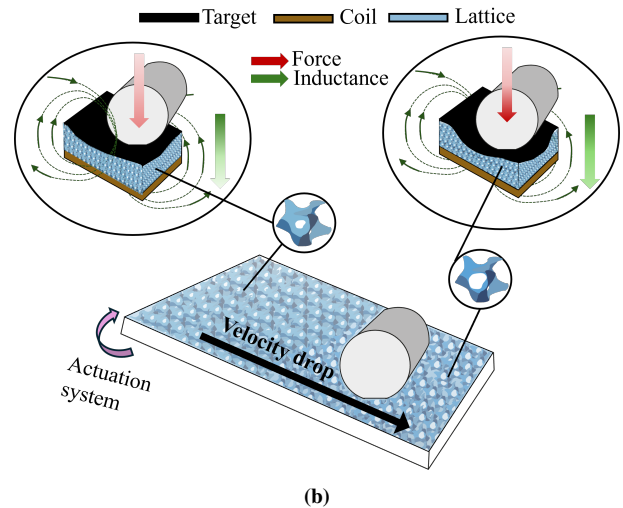
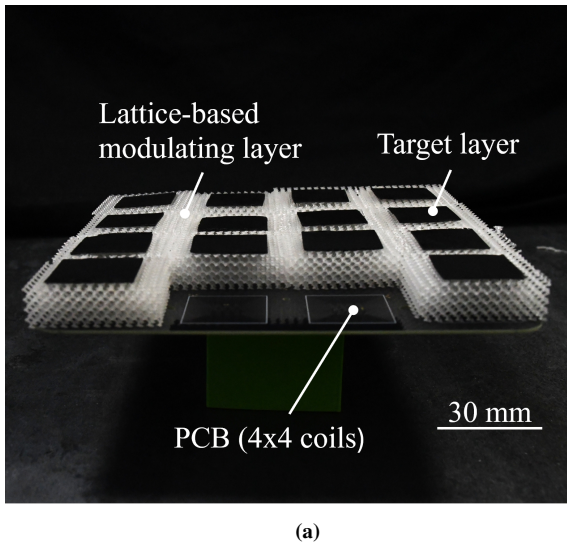


Fig. 1: Overview of the proposed COPESS-based surface manipulation system. (a) Photograph of the COPESS-based surface manipulation setup, consisting of a sensing unit with a 4x4 coil array, a lattice-based modulating layer, and a target layer. (b) Schematic illustration of the COPESS-based manipulation mechanism. The sensorized tile is covered with a 3D-printed lattice structure, which acts as a modulating layer. As the object transitions from a high-stiffness lattice to a low-stiffness lattice region, its velocity decreases while the sensor response increases.

- The modulating layer consists of compliant lattices, which deform under the applied pressure, changing the distance between the coils and the target layer.
- An array of 4x4 coils, made of four layers and with a dimension of 25 mm x 25 mm. The sensing tile consists of 16 coils, which are connected to 4 LDC1614 inductance-to-digital converter (Texas Instruments), which records the data with I2C protocol. The coils are excited by an Alternating Current (AC) and generate a dynamic magnetic field. An additional layer of ferrite at the bottom is used to provide Electromagnetic (EM) shielding [18].

Compression tests (0.5 mm/s, max strain = 50%) are performed to choose the most suitable lattice structure. In particular, SchwarzD, Gyroid, and XCell strut-based lattices are compared. For a given set of characteristics (Cell size = 3 mm, 14.5 mm ϕ x 12 mm), the gyroid exhibits the highest stiffness and the largest strain range before densification (Figure 2a), suggesting a wider working range. Figure 2b shows the mechanical characterization of the gyroid compared to the typical curve seen for the lattices [19]. Notably, it is observed that the stress-strain curve no longer exhibits the typical stress plateau. This extended region can be injectively mapped against a sensor response. Once the lattice approaches densification, the response is unreliable. Therefore, the sensors are designed to operate in the region preceding densification.

The thickness of the modulating layer is a critical design parameter. Any given coil has an effective region where the EM field is strong enough to interact with the target. To ensure a predictable and near-linear relationship between object displacement and sensor output, we design the sensor to operate within the linear region of the coil's inductance-

distance curve. As characterized in Figure 2c, this linear region extends to approximately 12 mm. Therefore, we set the lattice thickness to 12 mm to maximize the operational range while maintaining high linearity and sensitivity. The planar area is set to the size of the coils. Therefore, the lattices are designed to be 37.5 \times 37.5 \times 12 mm.

A. Lattice Fabrication and Post-Processing

Vat Photopolymerization techniques, such as stereolithography (SLA), are well-suited for printing highly intricate lattices due to their high-resolution light-based curing. In this work, SLA (Formlabs 4) is used to print Elastic 50A V2 resin, selected for its good initial compliance (Shore hardness = 50A) and fast recovery from deformation. The printing parameters are as follows: perimeter, model, and support fill regions receive an energy dose of 38.40 mJ/cm², whereas the light intensity is set as 11.5 mW/cm², layer thickness is set at 0.1 mm. Once printed, the samples are washed in isopropanol for 20 min and post-cured via UV irradiation for 45 min at 70 °C in a Form Cure unit (Formlabs). Various combinations of the lattice parameters (cell size, relative density, thickness) are printed and characterized. However, it is observed that there are strict limits on the cell size (2.2 mm to 4 mm) and relative density (7% to 30%) based on the printability of the lattices. At higher relative densities, the material tends to form clumps, trapping uncured resin in the cell cavities, and if relative density is lower than 7%, the structure is unable to support itself against gravity.

III. RESULTS AND DISCUSSION

A. Characterization

The COPESS is characterised on a three-axis indentation setup. Two micrometric manual linear stages control the positions of the X and Y stages. An M-111.1DG translation

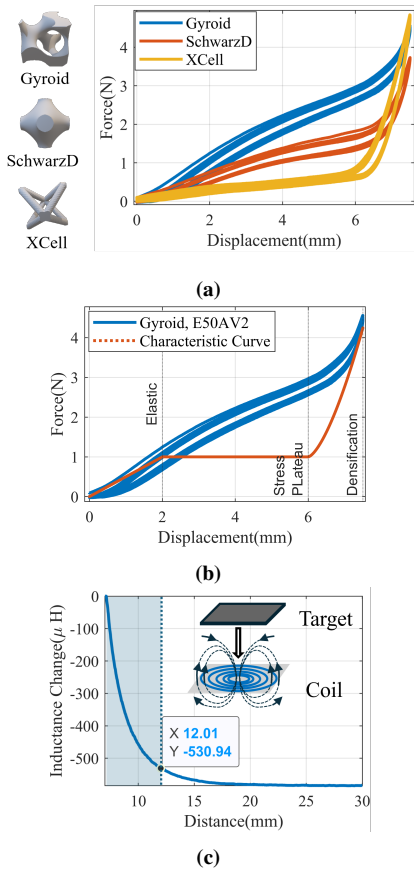


Fig. 2: Mechanical and electrical characterization informing the sensor’s design. (a) Force vs. displacement curves of three different lattice structures, demonstrating that the Gyroid (blue) offers the best combination of initial stiffness and strain range before densification. (b) Comparing a gyroid lattice structure printed using Elastic 50AV2 resin against the characteristic curve of a typical hyperelastic material. (c) Inductance change as a function of target distance, which heuristically determined the chosen thickness for the modulating lattice layer.

stage is positioned along the Z-axis above the X stage, which is controlled by the paired C-884.4DC motion controller (Physik Instrumente, USA). An ATI Nano17 (ATI Industrial Automation, USA) load cell is mounted on the Z stage. A plastic tape is placed on the tip of the metallic load cell (used as the indenter) to avoid interference with the ferromagnetic target. The inductance data is captured via the I2C protocol on the Arduino at a rate of 20 cycles per second using the open-source software CoolTerm. The force data from the load cell is recorded with the LabVIEW GUI. Both the inductance and force data are recorded at 20 Hz. To synchronize the data, each signal is first converted to a time-based data structure using its timestamp, and then synchronized using the nearest-neighbor interpolation method. This effectively aligns signals with different sampling rates or start times. This method provides an approximation that is reasonably precise for comparative analysis and preserves the relative timing accuracy between the two systems.

Preliminary tests characterizing various cell sizes (2.2 mm,

3 mm and 4 mm) and relative densities (7%, 10%, and 20%) within the available design space (based on printability limits) show that relative density is the biggest factor affecting the stiffness of a given lattice. Among the cell sizes tested, 3 mm showed a superior force range exceeding 2.2 mm by over 70% and 4 mm by 35% while maintaining similar sensitivity. Relative density refers to the percentage of the bounding volume containing the elastic material, with a smaller relative density resulting in a lattice of lower stiffness and vice versa. The gyroidal lattices are varied across three different relative densities and are subjected to cyclic compression tests. Specifically, the lattices of cell size 3 mm and relative densities of 7%, 10%, and 20% are chosen as they exhibited good repeatability across various prints. The sensorized tile is covered with lattice structures of uniform thickness. The lattice structure is compressed to 50% of its original height (12 mm), and the corresponding change in inductance is recorded.

Figures 3a–3c, show the inductance vs force curves of the selected lattices. Table I shows the resultant sensor characteristics from these configurations. The effective stiffness is calculated from the slope of the linear region (up to 2 mm displacement) of the force-displacement curves. The operational force range is defined as the maximum force measured at 6 mm compression. The sensitivity is calculated as the average slope of the inductance-force curves. The hysteresis is defined as the maximum difference between the loading and unloading curves expressed as a percentage of the full-scale inductance change. Increasing the relative density from 7% to 20% results in a 7-fold increase in stiffness and a 9-fold increase in operational force range, at the cost of a 23-fold decrease in sensitivity. This demonstrates a predictable design trade-off that allows for tailoring a sensor for specific applications. For applications requiring the delicate detection of lightweight objects like soft fruits, a low relative density (e.g., 7%) is ideal due to its high sensitivity. Conversely, for handling heavier, more robust objects, a higher relative density (e.g., 20%) provides the necessary force range and structural support. However, the results tend to vary over different lattices of the same characteristics due to minor printing defects.

It can also be observed that the mean values of the loading and unloading curves exhibit low hysteresis (8.7% for 20% relative density), which indicates good repeatability and improved accuracy during cyclic loading.

When sensors are positioned close to each other, there is a possibility of crosstalk, where the signal from one sensor interferes with its neighbours. To verify this, one sensor is activated while simultaneously recording the data from the adjacent sensors. Figure 4a shows no measurable effect on the neighbouring sensors, confirming that sensors don’t have an EM crosstalk. This demonstrates the electrical robustness of our design.

Lastly, the lattice sensors exhibit high repeatability in both inductance variation and mechanical characteristics. Figure 4b shows the results from cyclic testing over 200 cycles. The results at the beginning and end of the tests have

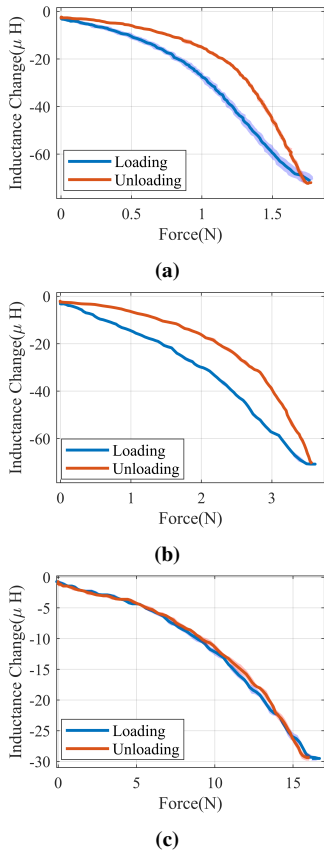


Fig. 3: Quantitative results demonstrating the co-design of mechanical and sensing properties by tuning lattice relative density. Inductance-force curves for (a) 7%, (b) 10%, and (c) 20% relative densities, illustrating how a higher relative density increases the operational force range at the cost of sensitivity (the slope of the curve). The data are presented as mean and confidence interval.

a 99.96% correlation overlap. The high repeatability of the sensor response demonstrates the mechanical robustness and durability of the 3D-printed gyroid structure. The material shows minimal degradation or plastic deformation, validating its suitability for applications involving repeated contact and loading.

B. Passive Object Guidance

Finally, i) the influence of these topologies on sensing in a moving platform; ii) the combination of different lattices on a sensor tile and its effect on sensing and motion of a given target object, are investigated. The tile is fixed to the end of a robotic arm (UR5e, Universal Robots, Denmark) using a custom 3D printed frame. The UR5 tilts the tile in a controlled manner. To showcase COPESS's sensing ability in versatile conditions, two different objects are manipulated: A rigid standard 500 g weight and an irregularly shaped soft object cast with silicon. In the first set of experiments, the tile is covered with lattice structures of relative density (7%) and tilted to $\pm 20^\circ$ at $0.2^\circ/\text{s}$ so that the object can move from one edge of the tile to the other. The sensor responses are recorded in a LabVIEW GUI, as shown in the video at 0:54. At lower inclination angles, the

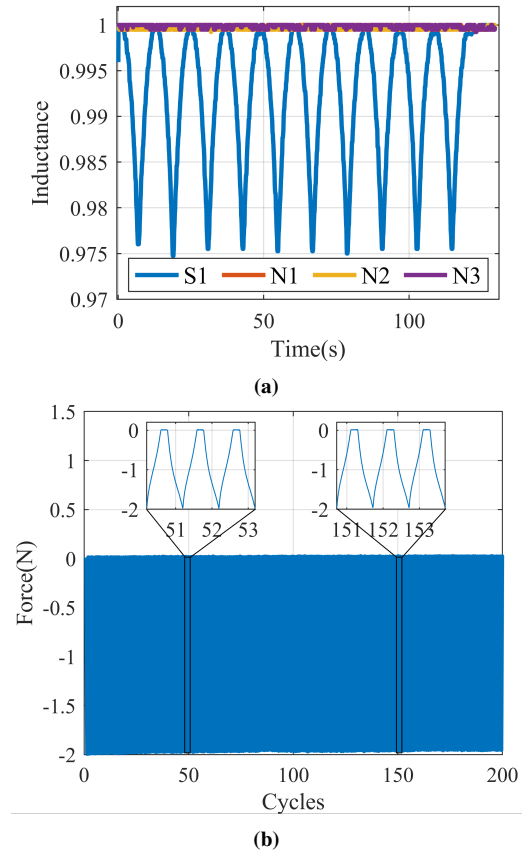


Fig. 4: Experimental validation of the sensor's robustness. (a) EM crosstalk when a linear vertical force is applied on S1 and the corresponding sensor response from its three neighbouring sensors. (b) Results from a 200-cycle mechanical repeatability test. The 99.96% overlap between the first three and last three cycles (inset) demonstrates the high durability and minimal plastic deformation of the 3D-printed gyroid structure.

object remains stable on the sensor and highly compresses the lattice, resulting in a more pronounced sensor response. As the angle increases, however, the object begins to roll, gaining speed. When passing over the sensors at higher velocities, the object has less time to compress the lattice, leading to a weaker response. Nevertheless, the sensor resolution is sufficient to determine the object's position. This experiment thus validates the soft surface's capability to provide localised sensing of objects during manipulation (Figure 5) and, eventually, to retrieve the object's velocity from the sensors' responses. Additionally, the results show that the sensing response is only dependent on the objects' weight and not affected by their shape or stiffness (which, on the other hand, affect the movement trajectory).

In the next set of experiments, the tile is covered with lattices with a 7% relative density on half of its area and the other half with a 10% relative density. The object is then moved from one edge of the tile to the other, as in the previous tests. When the object enters the 7% region, it moves more slowly because the lower stiffness leads to larger compressions due to the object's load. Greater compression

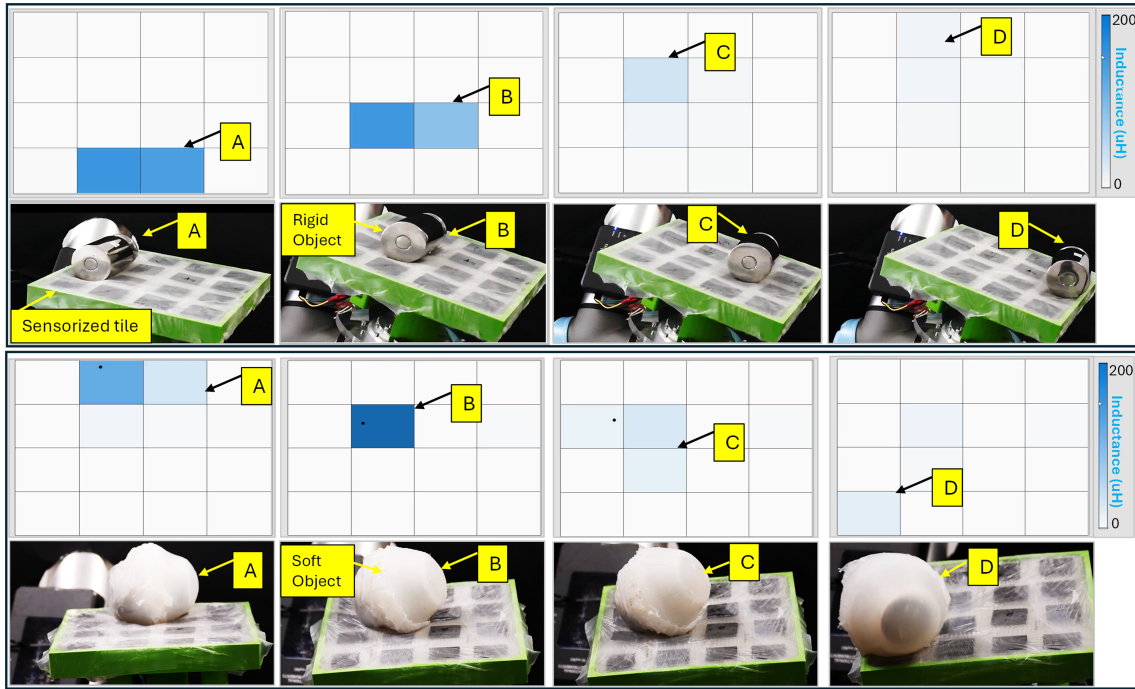


Fig. 5: Localized sensing and passive guidance of a manipulated object. The object is moved across the sensorized surface as it transitions from a low-stiffness region to a high-stiffness region, with its position tracked in a LabVIEW GUI. Two types of objects are demonstrated: Top Row: Rigid standard weight, Bottom Row: Irregular soft object

TABLE I: Quantified Performance Metrics Demonstrating the Co-Design of Mechanical and Sensing Properties. Each value represents the mean of $N = 5$ cyclic compression tests per lattice configuration.

Lattice Relative Density (%)	Effective Stiffness (N/mm)	Operational Force Range(N)	Sensitivity ($\mu\text{H/N}$)	Hysteresis (%)
7	0.37	1.78	39.04	20.07
10	0.54	3.61	18.92	17.00
20	2.52	16.68	1.70	8.70

also results in a stronger sensor response. In contrast, when the object transitions to the 10% region, the object moves more quickly, and the sensor response is weaker than in other sections. To further demonstrate passive object guidance, the object is given an initial impulse manually, and an overhead camera records the object's motion as shown in the video at 1:19. The surface is covered with each relative density combination individually, and the velocity and the distance traveled are obtained using an OpenCV script. Figure 6a shows the velocity plots along three different lattice stiffness regions. As the object rolls over the 20% region, the velocity is maintained with a slow deceleration. When the object interacts with the 10% region, it gains acceleration initially but eventually starts decelerating and stops after traveling approximately 110 mm. On the other hand, in the 7% region, the object decelerates after covering a short distance (75 mm) because of higher compliance. Figure 6b shows the same experiment on a tile covered with lattices of different stiffness. On transitioning from a 20% region to a 7% region, the velocity drops suddenly.

The influence of the lattice stiffness on the required actuation effort is also evident. To initiate motion on the stiffest uniform surface (20% relative density), a tilt angle of only

5° is required, whereas the much softer 7% surface needed a significantly larger tilt angle of 12.7° to overcome the higher initial stiction and rolling resistance, quantitatively demonstrating the direct link between programmed stiffness and the energy required for manipulation. These findings confirm that the motion of an object can be modulated by varying the stiffness of the COPESS layer, thereby highlighting the potential to passively guide objects in specific directions for practical applications, such as food packaging. Overall, the results offer promising avenues to design motion pathways that control an object's trajectory and relative velocity while improving actuator energy efficiency.

IV. CONCLUSIONS

In this study, a COPESS integrated with an inductive sensor array is proposed for use in soft surface manipulation. Gyroidal lattices printed via SLA form the deformable layer of the inductive sensor. The lattices are tuned by changing their relative density. The experiments demonstrate that by tuning the lattice stiffness, sensors with varying force ranges and sensitivities can be designed. The presented sensing platform demonstrates consistent and repeatable performance, even during the manipulation of soft and irregular objects, while maintaining a strong sensing response over a wide

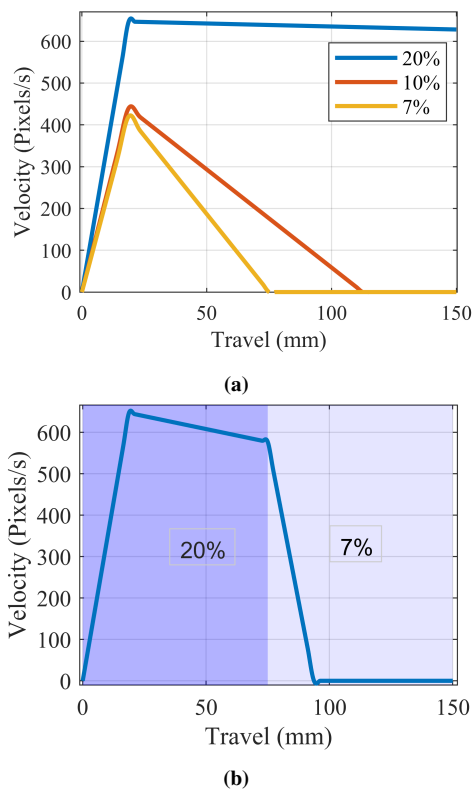


Fig. 6: Object velocity and travel distance on tiles with varying relative densities. (a) The 20 % region, being stiffer, exhibits lower friction, allowing continuous motion, whereas lower relative densities increase friction and cause faster deceleration. (b) Passive guidance of the object across regions with different relative densities. In the 20 % region, the object maintains motion with minor velocity drops, while in the 7 % region, it comes to rest rapidly due to higher friction.

force range. Moreover, we employ the inductive sensor as a force sensor, which lead to a larger inductance variation over a broad force range compared to previously reported inductive sensors, either using silicones [20] or 3D printed lattices [21] as modulating layers. The design of lattice structures is constrained by printability limitations and sensor performance. More efforts will be needed to extend the force working range while preserving high sensitivity. A more extensive study of other lattice structures and materials can be a future avenue of research. Additionally, the system is shown to effectively track an object's position and relative velocity on a moving platform regardless of the objects' characteristics. Lastly, the effect of combining lattices of different stiffnesses on actuation is studied. The results presented here offer many promising avenues for the use of lattices in soft handling systems. Future work includes devising a feedback mechanism to aid actuation and actively control the stiffness of the lattice structures.

REFERENCES

- [1] Z. Wang and S. Hirai, *Food Manipulation Technology: A Soft Robotics Approach*. CRC Press, 2025.
- [2] T. Wang, J. Zhang, J. Hong, and M. Y. Wang, "Dielectric elastomer actuators for soft wave-handling systems," *Soft robotics*, vol. 4, no. 1, pp. 61–69, 2017.
- [3] Z. Deng, M. Stommel, and W. Xu, "A novel soft machine table for manipulation of delicate objects inspired by caterpillar locomotion," *IEEE/ASME Transactions on Mechatronics*, vol. 21, no. 3, pp. 1702–1710, 2016.
- [4] P. Ingle, K. Støy, and A. Faiña, "Soft manipulation surface with reduced actuator density for heterogeneous object manipulation," in *2025 IEEE 8th International Conference on Soft Robotics (RoboSoft)*. IEEE, 2025, pp. 1–8.
- [5] Z. Xue, H. Zhang, J. Cheng, Z. He, Y. Ju, C. Lin, G. Zhang, and H. Xu, "Arraybot: Reinforcement learning for generalizable distributed manipulation through touch," in *2024 IEEE International Conference on Robotics and Automation (ICRA)*. IEEE, 2024, pp. 16 744–16 751.
- [6] Z. Wang, S. Demirtas, F. Zuliani, and J. Paik, "Surface-based manipulation with modular foldable robots," *npj Robot*, vol. 4, 2026. [Online]. Available: <https://doi.org/10.1038/s44182-025-00069-6>
- [7] M. Awais, E. AliAbbasi, A. Y. Atik, M. J. Bathaei, M. Ali, R. Das, C. Dag, A. Ullah, R. Singh, K. S. Turker *et al.*, "Multiplexed piezoelectric electronic skin with haptic feedback for upper limb prosthesis," *Advanced Sensor Research*, vol. 3, no. 12, p. 2400100, 2024.
- [8] S. Yun, S. Park, B. Park, Y. Kim, S. K. Park, S. Nam, and K.-U. Kyung, "Polymer-waveguide-based flexible tactile sensor array for dynamic response," *Advanced Materials (Deerfield Beach, Fla.)*, vol. 26, no. 26, pp. 4474–4480, 2014.
- [9] S. Chen, S. Li, Y. Zheng, B. Fong, Y. Li, P. Dong, D. Hwang, and S. Yao, "Highly sensitive and robust soft tri-axial tactile sensors enabled by dual inductive sensing mechanisms," *Soft Science*, vol. 5, no. 1, pp. N–A, 2025.
- [10] H. Wang, J. Kow, G. de Boer, D. Jones, A. Alazmani, and P. Culmer, "A low-cost, high-performance, soft tri-axis tactile sensor based on eddy-current effect," in *2017 IEEE SENSORS*, 2017, pp. 1–3.
- [11] H. Wang, J. Kow, N. Raske, G. De Boer, M. Ghajari, R. Hewson, A. Alazmani, and P. Culmer, "Robust and high-performance soft inductive tactile sensors based on the eddy-current effect," *Sensors and Actuators A: Physical*, vol. 271, pp. 44–52, 2018.
- [12] D. Jones, A. Alazmani, and P. Culmer, "A soft inductive tactile sensor for slip detection within a surgical grasper jaw," in *2019 IEEE SENSORS*. IEEE, 2019, pp. 1–3.
- [13] S. Hamaguchi, T. Kawasetsu, T. Horii, H. Ishihara, R. Niiyama, K. Hosoda, and M. Asada, "Soft inductive tactile sensor using flow-channel enclosing liquid metal," *IEEE Robotics and Automation Letters*, vol. 5, no. 3, pp. 4028–4034, 2020.
- [14] O. Ozioko, M. Hersh, and R. Dahiya, "Inductance-based soft and flexible pressure sensors using various compositions of iron particles," in *2019 IEEE SENSORS*. IEEE, 2019, pp. 1–4.
- [15] D. Cafiso, F. Bernabei, M. Lo Preti, S. Lantean, I. Roppolo, C. F. Pirri, and L. Beccai, "Dlp-printable porous cryogels for 3d soft tactile sensing," *Advanced Materials Technologies*, vol. 9, no. 10, p. 2302041, 2024.
- [16] B. Dacre, N. Bessone, M. L. Preti, D. Cafiso, R. Moreno, A. Faiña, and L. Beccai, "Neural cellular automata for decentralized sensing using a soft inductive sensor array for distributed manipulator systems," *arXiv preprint arXiv:2502.01242*, 2025.
- [17] Z. Dong, Q. Xu, J. Tu, Y. Zhu, J. Li, Y. Hu, H. Ren, P. Dong, X. Cheng, and Z. Xue, "A dual-layer reverse-helical inductive wireless passive flexible temperature sensor integrated with ferrite for bearings monitoring," *IEEE Sensors Journal*, 2025.
- [18] M. Maaß, A. Griessner, V. Steixner, and C. Zierhofer, "Reduction of eddy current losses in inductive transmission systems with ferrite sheets," *Biomedical engineering online*, vol. 16, no. 1, p. 3, 2017.
- [19] C. W. Haney and H. R. Siller, "Properties of hyper-elastic-graded triply periodic minimal surfaces," *Polymers*, vol. 15, no. 23, 2023. [Online]. Available: <https://www.mdpi.com/2073-4360/15/23/4475>
- [20] H. Wang, M. Totaro, A. A. Blandin, and L. Beccai, "A wireless inductive sensing technology for soft pneumatic actuators using magnetorheological elastomers," in *2019 2nd IEEE international conference on soft robotics (RoboSoft)*. IEEE, 2019, pp. 242–248.
- [21] R. Bhaumik, T. Preindl, A. Ion, C. Ayala-Garcia, N. Cohen, M. Haller, and N. Münzenrieder, "Inductive pressure sensors using 3d-printed structures with tunable stiffness," *IEEE Sensors Letters*, 2025.